

Hybridization Trends for Main Group Elements and Expanding the Bent's Rule Beyond Carbon: More than Electronegativity

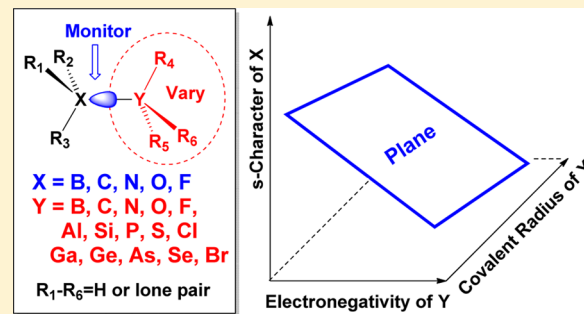
Igor V. Alabugin,*† Stefan Bresch,† and Mariappan Manoharan‡

†Department of Chemistry and Biochemistry, Florida State University, Tallahassee, Florida 32306-4390, United States

‡School of Science, Engineering and Mathematics, Bethune Cookman University, Daytona Beach, Florida 32114, United States

Supporting Information

ABSTRACT: Trends in hybridization were systematically analyzed through the combination of DFT calculations with NBO analysis for the five elements X (X = B, C, N, O, and F) in 75 H_nX-YH_m compounds, where Y spans the groups 13–17 of the periods 2–4. This set of substrates probes the flexibility of the hybridization at five atoms X through variations in electronegativity, polarizability, and orbital size of Y. The results illustrate the scope and limitations of the Bent's rule, the classic correlation between electronegativity and hybridization, commonly used in analyzing structural effects in carbon compounds. The rehybridization effects are larger for fluorine- and oxygen-bonds than they are in the similar bonds to carbon. For bonds with the larger elements Y of the lower periods, trends in orbital hybridization depend strongly on both electronegativity and orbital size. For charged species, the effects of substituent orbital size in the more polarizable bonds to heavier elements show a particularly strong response to the charge introduction at the central atom. In the final section, we provide an example of the interplay between hybridization effects with molecular structure and reactivity. In particular, the ability to change hybridization without changes in polarization provides an alternative way to control structure and reactivity, as illustrated by the strong correlation of strain in monosubstituted cyclopropanes with hybridization in the bond to the substituent.



INTRODUCTION

Hybridization. Hybridization of atomic orbitals, a fundamental concept introduced by Pauling,^{1,2} describes mixing of orbitals at an atom which adds directionality to the Lewis-shared electron pair/chemical-bond concept. Although the undergraduate textbook description rarely ventures far beyond the standard cadre of sp³, sp², and sp-hybridization models, any percentage of s character in a hybrid orbital within the 0–100% range is physically possible. Consequently, the hybridization parameter λ in sp² orbitals at a carbon atom can adopt any value from zero (a pure s orbital) to infinity (a pure p orbital), depending on the particular bonding situation. The only limitation is that the total s and p character in all occupied orbitals should add up to 100% and 300%, respectively, reflecting the fact that carbon hybrid orbitals are made from one s orbital and three p orbitals.³

Conceptually, hybridization can be described using the combination of electron promotion and orbital mixing, as shown in Figure 1. Although promotion of valence s electrons to the respective p subshell is energetically unfavorable since it leads to an excited state, this cost of excited state formation is compensated by the subsequent formation of stronger chemical bonds made possible by the shape and directionality of a newly available set of hybrid orbitals. Since hybrid orbitals are simply a linear combination of the original atomic orbitals (AOs), their formation (hybridization per se) at an isolated atom is just a mathematical operation that does not involve an energy cost.

This model illustrates both the cost paid for the involvement of low energy s electrons in chemical bonding and the role of hybridization as a mechanism in maximizing chemical bonding.

Even though hybridization has been in the center of many seeming discrepancies between MO and VB theories (i.e., photoelectron spectrum of methane and “rabbit ears” lone pairs of water^{5,6}), such discrepancies have been successfully resolved. A recent suggestion, to remove hybridization from the undergraduate textbooks^{8,7} was met with a resounding opposition.^{8–11}

Bent's Rule. This link between hybridization and other parameters describing the atom or molecule, such as geometry, energies, and spectroscopic properties, is dynamic: external or internal perturbations affect the hybridization and the associated parameters.^{12,13} A “minor” change in hybridization can result in dramatic changes in chemical properties, which can be directly probed experimentally through secondary kinetic isotope effects.^{14–17}

The utility of hybridization-based structural analysis in organic chemistry is greatly expanded by the well-established connection of hybridization and electronegativity, known as Bent's rule.^{18–20} This rule states that s character concentrates in orbitals directed toward electropositive substituents or, alternatively, that atoms

Received: March 11, 2014

Revised: April 27, 2014

Published: April 28, 2014

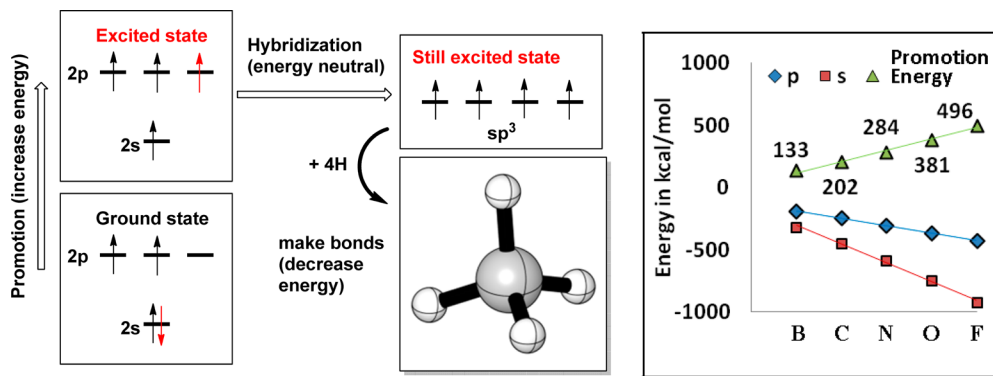


Figure 1. Left: sequence of electron promotion and orbital mixing for carbon atoms. Right: energy of the p orbitals (blue ♦), s orbitals (red ■), and the promotion energy (green ▲) for B, C, N, O, and F. As the promotion energy rises, the importance of hybridization is expected to decrease. Values from ref 4.

direct hybrid orbitals with more p character toward more electronegative elements. Earlier computational analysis found an excellent correlation between the hybridization at carbon and the electronegativity of Y in C–Y bonds of monosubstituted alkanes,^{12,13} alkenes, and alkynes.¹³

Although Bent's rule explains a wide variety of rehybridization effects used in control of reactivity in organic compounds,^{21–52} the correlation of hybridization and electronegativity has not been widely useful for noncarbon systems (except for a few notable exceptions,^{20,53–64} especially the recent extension to transition metal compounds).^{55–57}

A broad study which would utilize the modern computational methods in order to test the general applicability of Bent's rule to main group elements other than carbon and correlate trends in orbital hybridization with observable electronic and structural parameters can be beneficial for the development of a more unified foundation of structural chemistry. Filling this gap will provide a framework for structural analysis of a large variety of molecular systems throughout the periodic system.

Scope. This work presents trends in hybridization of B, C, N, O, and F in H_nX-YH_m compounds, where the atom X belongs to the second period of the periodic table and the atom Y spans groups 13–17 of the periods 2–4. Use of H atoms allowed us to concentrate on the properties of the central X–Y bond in a consistent manner. The choice of systems will allow us to probe the flexibility of the hybridization at five different atoms, X, through variations in electronegativity, polarizability, and orbital size of Y.^{65,66} Since we concentrate on classic 2c,2e-bonding, we did not include 3c,2e-bonded nonclassical structures more typical for the Group III compounds (see Figure 2).

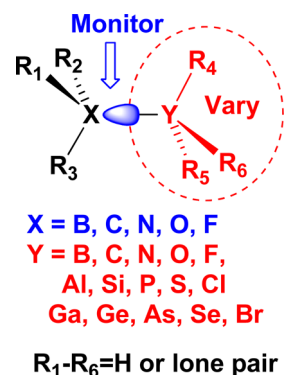


Figure 2. Scope of this paper.

COMPUTATIONAL DETAILS AND CHOICE OF METHOD

All structures were fully optimized at the MP2/6-311++G**, B3LYP/6-311++G**, and M06-2X/aug-cc-pVTZ levels of theory using Gaussian software.^{67,68} Electronic structures of model compounds (H_nX-YH_m ; $H_nX = BH_2, CH_3, NH_2, OH$, and F and $YH_m = F, Cl, Br, OH, SH, SeH, NH_2, PH_2, AsH_2, CH_3, SiH_3, GeH_3, BH_2, AlH_2$, and GaH_2)⁶⁹ were studied by performing natural bond orbital (NBO) analysis^{70–82,83} with NBO 4.0.⁸⁴ Detailed descriptions of the NBO calculations are available in the literature.^{85–87} All geometries were confirmed to be energy minima by frequency analysis. However, we have not carried out extensive searches for the global minima. The hybridization parameters obtained from DFT and MP2 are in a good agreement with each other. The B3LYP/6-311++G** method has been used for the discussion throughout this paper.

Hybridization was quantified through natural bond orbital (NBO) analysis. The advantage of NBO is that this method makes no a priori assumption about orbital hybridization. Instead, it analyzes the wave function or electron density by finding the most rapidly converging set of localized orbitals (NBOs) closely tied to the classic bonding concepts. This process involves sequential transformations of nonorthogonal atomic orbitals (AOs) to the sets of “natural” atomic orbitals (NAOs), hybrid orbitals (NHOs), and bond orbitals (NBOs). Each of these localized basis sets is complete and orthonormal. As shown by Weinhold and co-workers,⁸⁹ the NHOs are in excellent agreement with the predictions based on both electronegativity and bond angles and, thus, provide an accurate tool for computational studies of hybridization. In addition, because each NBO corresponds to a linear combination of hybrid orbitals, the square of orbital coefficients in this combination reflects polarization of the respective bonds. In summary, NBO is an ideal theoretical method for probing the connection between bond hybridization and polarization embodied by Bent's rule.

RESULTS AND DISCUSSION

Bent's rule connects electronegativity with hybridization. In order to gain further insights into the role of electronegativity on the properties of X–Y covalent bonds, we analyzed the correlations of X–Y bond polarization and hybridization of X with Pauling's electronegativity of element Y.

Bond Polarization as a Function of Partner's Electronegativity. The changes in bond polarization summarized in Figure 3 and Table 1 are large from the very polar F–Al (92% at F)

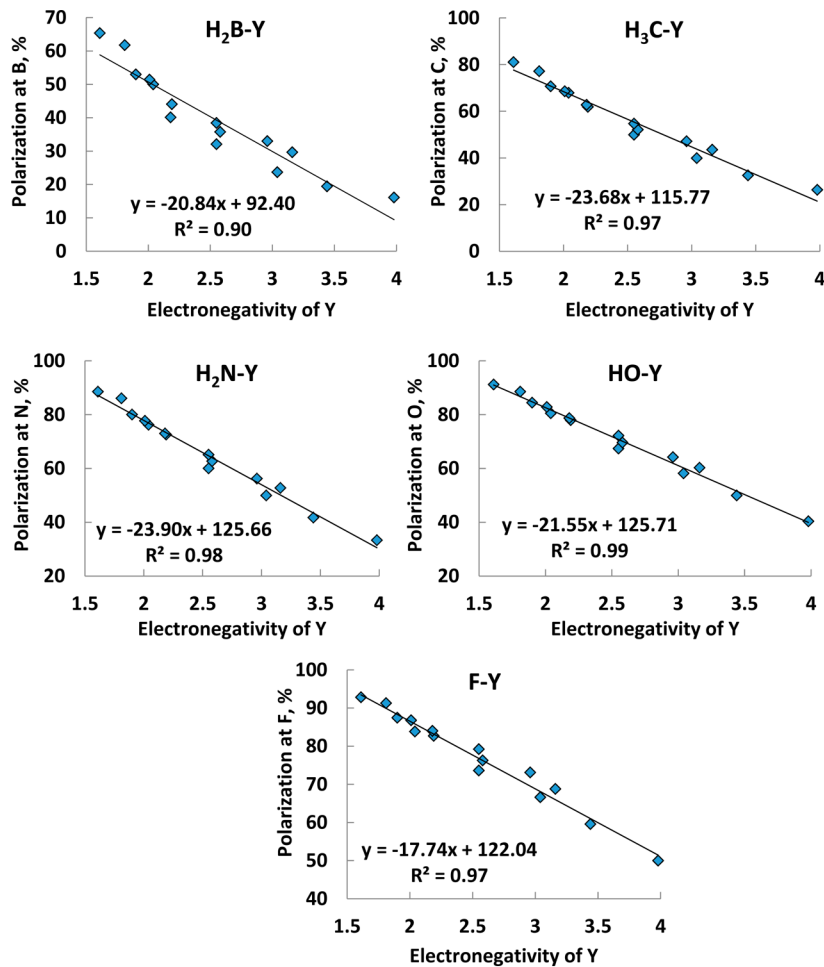


Figure 3. Correlation of the Pauling electronegativity of Y in the substituted H_nB-Y, H₃C-Y, H₂N-Y, HO-Y, and F-Y systems with the polarization at B, C, N, O, and F in the corresponding X-Y bonds at the MP2/6-311++G(d,p) level of theory.

Table 1. Polarization (Pol) of the X-Y Bond in H_nX-YH_m Systems (H_nX = H₃C, H₂N, HO, and F; Y = F, Cl, Br, OH, SH, SeH, NH₂, PH₂, AsH₂, CH₃, SiH₃, GeH₃, BH₂, AlH₂, and GaH₂) Calculated at the MP2 Level^a

H _n X-YH _m	Pol (B) _{B-Y} (%)	Pol (C) _{C-Y} (%)	Pol (N) _{N-Y} (%)	Pol (O) _{O-Y} (%)	Pol (F) _{F-Y} (%)
H _n X-BH ₂	50.00	67.93	76.28	80.54	83.88
H _n X-CH ₃	32.07	50.00	60.04	67.42	73.65
H _n X-NH ₂	23.72	39.96	50.00	58.22	66.63
H _n X-OH	19.46	32.58	41.78	50.00	59.60
H _n X-F	16.12	26.35	33.37	40.40	50.00
H _n X-AlH ₂	65.38	81.07	88.58	91.23	92.86
H _n X-SiH ₃	52.98	70.75	80.07	84.50	87.48
H _n X-PH ₂	44.09	61.90	72.60	77.96	82.74
H _n X-SH	35.78	52.15	62.74	69.64	76.28
H _n X-Cl	29.67	43.56	52.79	60.31	68.83
H _n X-GaH ₂	61.78	77.22	86.11	88.56	91.31
H _n X-GeH ₃	51.42	68.58	77.76	82.87	86.81
H _n X-AsH ₂	40.14	62.78	73.03	78.76	84.02
H _n X-SeH	38.46	54.72	65.14	72.22	79.24
H _n X-Br	33.02	47.18	56.28	64.23	73.14

^aPolarization is calculated as the square of NHO coefficients in the X-Y NBOs. Each of the values can be taken as the percentage of electron density at X in the X-Y bonds at the MP2/6-311++G(d,p) level of theory. See the Supporting Information for the additional data at other levels of theory.

bond to the nonpolar bonds of symmetric compounds (B-B, C-C, N-N, etc.). For every X in the broad selection of X-Y bonds studied in this work, the correlation between NBO polarization and electronegativity⁸⁸ is linear over the wide range of electronegativities. The correlation coefficients of >0.9 supports the physical accuracy of NBO dissections.

Bond Hybridization as a Function of Partner's Electronegativity. Computed values of s character in the hybrid orbital of X in H_nX-YH_m compounds are summarized in Table 2. These values illustrate a considerable range of hybridization parameters: from 5% s character in the ~sp²⁰ hybrids, forming the F-F bond of molecular fluorine to ~49% at N in the N-Al bond.

The correlations of the s character of X in H₂B-YH_m, H₃C-YH_m, H₂N-YH_m, HO-YH_m, and F-YH_m bonds with the electronegativity of Y are graphically presented in Figure 4 (see the Supporting Information for more detailed presentation). The NBO analysis shows that the % s character on X (B, C, N, O, and F) atom found in the H_nX-YH_m systems varies significantly (26–35%, 18–33%, 12–49%, 8–48%, and 5–44%, respectively). However, in every case, the s character of the X atom-centered hybrid orbital in an X-Y bond successively decreases with the increase in electronegativity of the substituent Y. This trend clearly follows Bent's rule and illustrates how this rule applies to other elements.

Interestingly, this correlation is linear only for carbon and boron but not for X = N, O, and F. In the latter cases, the hybridization of X shows a much stronger nonlinear response to

Table 2. S-Character (s-char) of Hybrid Atom X at the X–Y Bond in H_nX-YH_m Systems ($H_nX = H_2B, H_3C, H_2N, HO$, and F; $YH_m = F, Cl, Br, OH, SH, SeH, NH_2, PH_2, AsH_2, CH_3, SiH_3, GeH_3, BH_2, AlH_2$, and GaH_2) Calculated at the MP2/6-311+G(d,p) Levels^a

H_nX-YH_m	s-char (B) _{B-Y} (%)	s-char (C) _{C-Y} (%)	s-char (N) _{N-Y} (%)	s-char (O) _{O-Y} (%)	s-char (F) _{F-Y} (%)
H_nX-BH_2	36.03	33.07	47.84	45.69	44.09
H_nX-CH_3	34.66	29.82	32.36	30.01	27.73
H_nX-NH_2	30.73	26.54	26.61	19.54	16.41
H_nX-OH	28.69	23.53	18.61	12.42	9.56
H_nX-XF	27.27	20.79	14.34	8.09	5.33
H_nX-AlH_2	35.39	30.17	50.14	50.05	49.01
H_nX-SiH_3	34.90	29.86	41.35	42.27	42.40
H_nX-PH_2	33.78	26.67	34.14	28.14	27.01
H_nX-SH	31.52	24.13	24.57	19.25	16.18
H_nX-Cl	29.54	21.57	16.74	11.54	9.33
H_nX-GaH_2	34.55	27.26	44.25	34.92	33.81
H_nX-GeH_3	34.02	27.32	33.18	31.55	30.15
H_nX-AsH_2	30.88	24.54	28.09	22.50	21.99
H_nX-SeH	31.02	22.34	21.15	16.22	14.67
H_nX-Br	29.21	20.23	14.93	10.52	9.38

^aSee the Supporting Information for the additional data at other levels of theory.

changes in electronegativity of Y. As a result, during the “Y scan” in each of the three periods (Y = group 3 → ⋯ → group 7), X = C, and B start (in their bonds to B, Al, and Ga) with the least amount of s character but end up (in their bonds to F, Cl, and Br) with the most amount of s character among the five choices of X. This divergence reflects the range of possible hybridization values, which for X = N, O, and F, is much larger than it is for C and B (see Figure 5).

The greater sensitivity of hybridization of N, O, and F to the variations in the nature of their bond-forming partner in the X–Y bonds suggests the potentially increased importance of Bent’s rule for the chemistry of these elements. We will discuss the reasons for this interesting behavior in one of the subsequent sections. However, before that, we will analyze an even more important effect that affects the generality of hybridization trends across the periodic table.

Atomic Size Effects on Bond Hybridization. Unlike the uniform trend in X–Y polarization, hybridization of atom X in

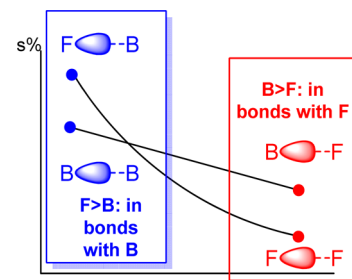


Figure 5. Hybridization capabilities for atoms with and without lone pairs. Note that F displays much greater rehybridization than B.

the X–Y bonds does not obey a single correlation with electronegativity of Y for the full range of Y across the periodic table. A good correlation between hybridization of atom X (B, C, N, O, and F) in the families of H_nX-YH_m molecules and electronegativity of Y is only observed for Y from the same period (Figure 6). The hybridization patterns clearly change upon transition between the periods.

The observed absence of global correlation between s character of X and electronegativity of Y, which involves atoms Y from all three rows suggests the presence of an additional factor, which changes hybridization of X as it forms bonds to atoms Y from different periods (e.g., BH_2 , AlH_2 , and GaH_2).

The high-quality global correlation in Figure 3 above clearly suggests that this factor is not the X–Y bond polarity. For each given X in the X–Y bond, the calculated bond polarity clearly correlates with electronegativity of Y.

The correlation curves for Y from the three periods are roughly parallel, which means that each of the X elements rehybridizes in a qualitatively similar way in response to the change in electronegativity of element Y, but there is an abrupt, incremental change that separates data for the different periods (see Figure 6).

The missing factor needed to explain these trends is the difference in the size of atomic orbitals for elements Y from the three different periods. Since rehybridization is aimed at maximizing the chemical bonding, the central atom responds to an increase in the orbital size of its binding partner by allocating additional p character in the bond(s) directed toward the elements from the lower periods.

As illustrated by Figure 7, the two-parameter correlation of hybridization at carbon in C–Y bonds with electronegativity (E)

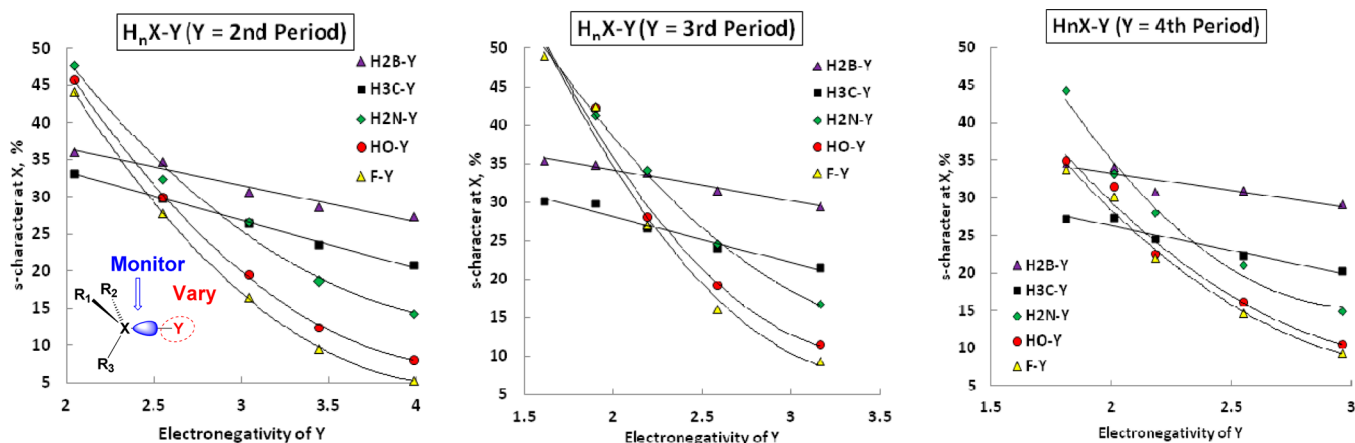


Figure 4. Correlations of the s character in the hybrid orbital of atom X (B, C, N, O, and F) in X–Y bonds in H_nX-YH_m compounds with the electronegativity of element Y for the periods 2–4 of the periodic table (see Figure S1 of the Supporting Information for a more detailed analysis). Calculations are based on the MP2/6-311+G(d,p) level.

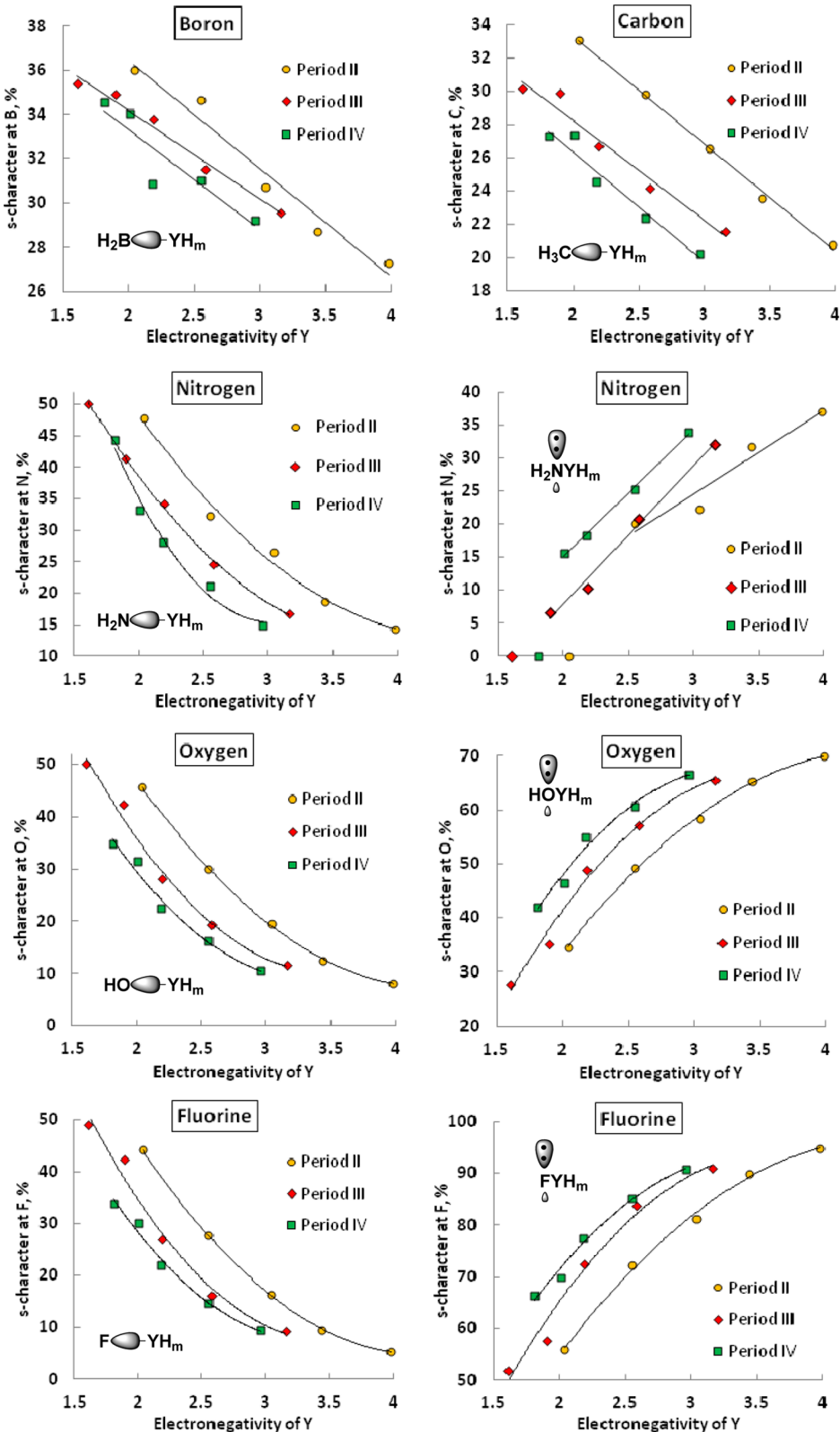


Figure 6. Correlations of s character in the hybrid orbital of each of the five atoms X (B, C, N, O, and F) in the X–Y bonds of $\text{H}_n\text{X}-\text{YH}_m$ compounds with electronegativity of element. For X = N, O, and F, the s character in the hybridized lone pair is shown on the right side. The remaining lone pairs in oxygen and fluorine are 100% p hybridized. Trend lines are linear or second-order polynomial. Calculations are based on the MP2/6-311++G(d,p) level.

and covalent radius (R) of element Y is excellent. Analogous correlations of equally good quality were found for all five elements X (B, C, O, N, and F) analyzed in this work (see Figures S1–S4 of the Supporting Information and Figure 8).

The relative importance of electronegativity and orbital size in each correlation reflects the unique balance of these two factors in determining the hybridization trends observed for each element, as shown in Table 3. The ability of the atoms to

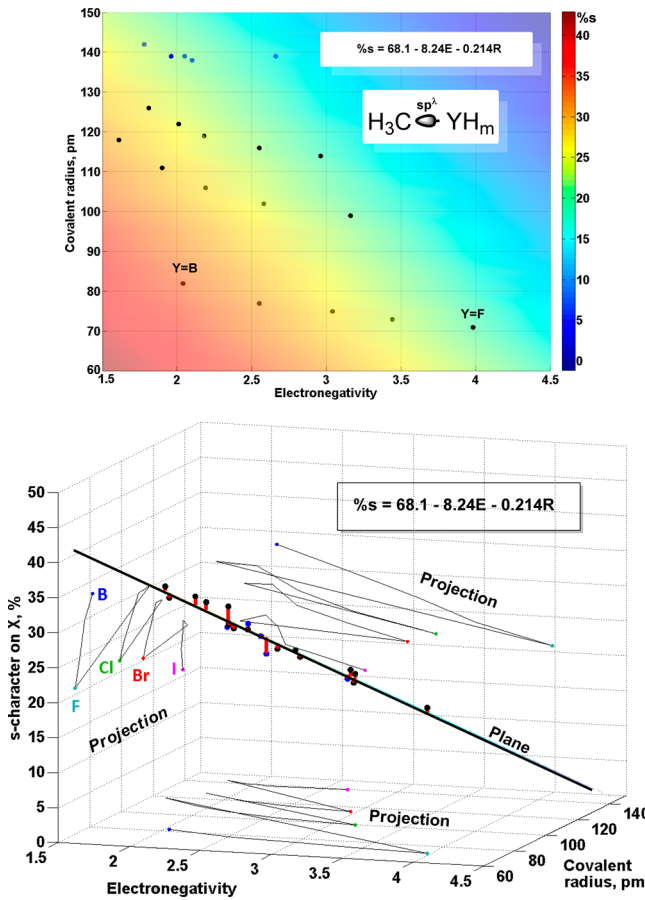


Figure 7. s-Character (%), color coded according to the scale shown) of the hybrid orbital of carbon in C–Y bonds of $\text{H}_3\text{C}-\text{YH}_m$ compounds as a function of electronegativity (E) and covalent radius (R) of atom Y. Top: Top view on the fitted plane. Black: data points $Y = 2\text{nd}$ – 4th period. [(MP2/6-311++G(d,p)] Blue: data points $Y = 5\text{th}$ period. (MP2/Lan2LDZ). Bottom: view along the plane. Red: deviation of the data points from the fitted plane ($R^2 = 0.947$). The projections of the data points on the coordinate planes are shown as a zigzag chain of black line segments for the substituents $Y = \text{B}, \text{F}, \text{Cl}, \text{Br}$, and I . Note that none of the three projections (corresponding to a single parameter fit) can satisfactorily explain the hybridization trends.

rehybridize increases from left to right in the period. Both the electronegativity and the size coefficients (C_E and C_R , respectively) increase from B to F. However, this increase in the two contributions of these two sources of rehybridization is not perfectly synchronized. For example, the importance of orbital size is increased for carbon versus boron much more than the importance of electronegativity (C_E/C_R ratios 64 and 39). On the other hand, transition from carbon-to-nitrogen dramatically increases sensitivity of hybridization to electronegativity of substituent without having an equally large effect on its sensitivity to the orbital size. Overall, all atoms with lone pairs (N, O, and F) show much greater sensitivity to electronegativity than atoms without lone pairs (B and N). For the three atoms with lone pairs, sensitivities to electronegativity are large and change only slightly with the increased atomic charge. As a result, the relative importance of orbital size increases in the following order $\text{N} < \text{O} < \text{F}$. The relative contribution of the orbital size (as evaluated by the C_E/C_R ratio) is the largest for C and F.

Expansion to Central Atoms with Multiple Substituents of Different Nature. If the substitution pattern is changed from simple hydrogen atoms toward multiple different

substituents on the atom of interest X: $\text{H}_n\text{X}-\text{YH}_m \rightarrow \text{S}_i\text{S}_j\text{S}_k\text{X}-\text{YH}_m$, an alteration of the s character donated into the X–Y bond appears. To find an appropriate description, we computed 35 different substituted methane compounds $\text{CS}_i\text{S}_j\text{S}_k\text{S}_l$ (substituents S: F, Cl, Br, and H in all chemically distinct combinations) (see Figure 9). Analysis reveals that the s character of a particular bond can be described as

$$\%s_i = 25 - A \left(e_i - \frac{(e_j + e_k + e_l)}{3} \right) - B \left(c_i - \frac{(c_j + c_k + c_l)}{3} \right) \quad (1)$$

where e denotes the Pauling electronegativities of the substituents and c their corresponding covalent radius. The fit parameters A and B are 2.013 and 0.0433/pm and (i, j, k, and l) is any permutation of (1, 2, 3, and 4). The structure of the equation ensures that the total % s character is always 100% as well as a symmetric distribution of s character when the substituents are symmetric. This equation describes hybridization at any given bond at a multicovalent atom as a “tug of war” between electronegativities and orbital size effects in all bonds of this atom. Deviations from the correlation illustrate that this simple picture is only the first, sometimes crude, approximation (Figure 9).

HYBRIDIZATION VS GEOMETRY

Valence Angles. The relationship of the bond angle $\Theta_{ij}(i-X-j)$ between arbitrary atoms i and j out of n atoms bonded to an atom X, and the hybridization parameters λ_i and λ_j in sp^3 bonds follows eq 2 derived from Coulson’s Orthogonality Theorem:⁸⁹

$$1 + \sqrt{\lambda_1 \lambda_2} \cos(\Theta_{ij}) = 0 \quad (2)$$

Although bond angles do not always correspond to orbital angles (i.e., due to the formation of bent bonds⁹⁰), the H–X–Y bond angles follow eq 2 fairly well for all 60 compounds that include this type of bond angle (Figure 10).

Furthermore, the H–X–Y bond angles at nitrogen and oxygen can be directly derived from the s character in the X–Y (X = N and O) bond, even without knowing the s character in the corresponding N–H and O–H bonds (Figure 11). For boron and carbon bond angles, the correlation is poor, suggesting that other factors (i.e., hybridization changes in the X–H bond) contribute to the observed H–X–Y valence angles. Again, this observation illustrates the special properties of lone pairs as facilitators in reaching the optimal hybridization values for the chemical bond formation.

“SUPER-REHYBRIDIZATION” IN N–Y, O–Y, AND F–Y BONDS

As we discussed earlier, the range of hybridization values for X = N, O, and F is considerably larger than the range of hybridization values for X = B and C in their respective X–Y bonds. This interesting phenomenon suggests that the importance of rehybridization effects may increase for the more electronegative elements. In several sections given below, we illustrate the origins of this behavior. We will show below that it has several components: (a) the unimportance of hybridization in nonpolar X–X bonds of electronegative elements and (b) the presence of lone pair(s) with their increased ability to rehybridize and, in some cases (i.e., bonds with boron), participate in the formation of the X = B dative double bonds.

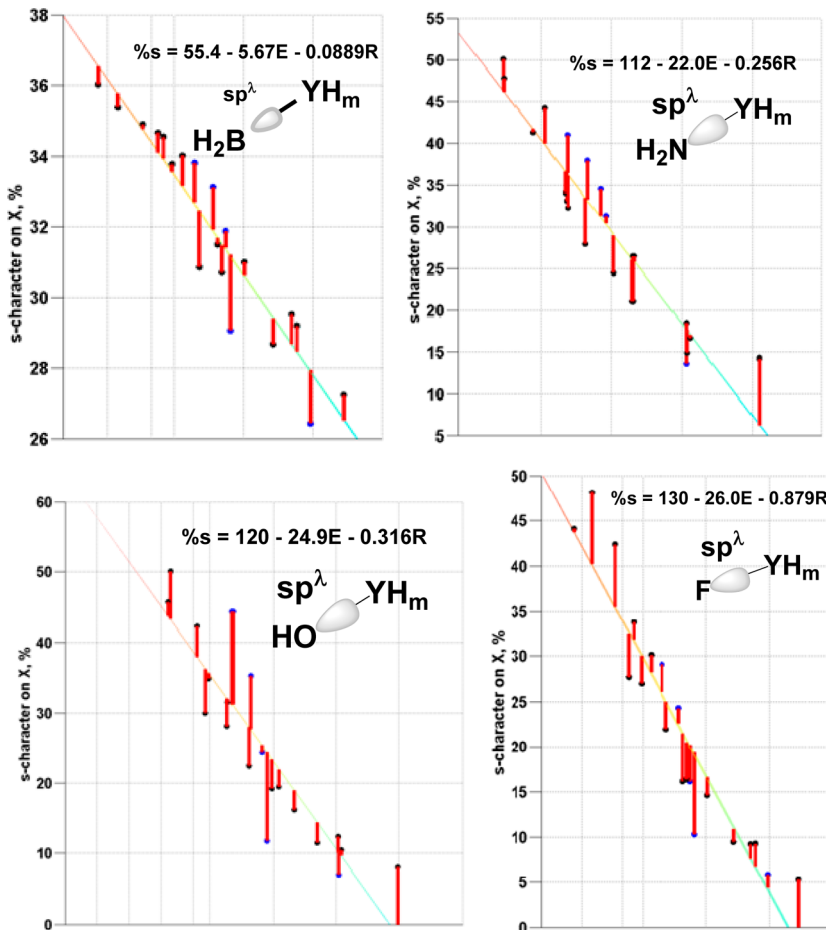


Figure 8. s Character (%) of the hybrid orbitals of B, N, O, and F in X–Y bonds of $\text{H}_n\text{X}-\text{YH}_m$ compounds as a function of electronegativity (E) and covalent radius (R) of atom Y. View along the plane. Red: deviation of the data points from the fitted plane. Full correlations analogous to Figure 7 are given in the Supporting Information.

Table 3. Coefficients for the Two-Parameter Correlations for B–Y, C–Y, N–Y, O–Y and F–Y bonds^a

system	C_E/C_R	fit equation
$\text{H}_2\text{B}-\text{YH}_m$	64	$\%s = 55.4 - 5.67E - 0.0889R$
$\text{H}_3\text{C}-\text{YH}_m$	39	$\%s = 68.1 - 8.24E - 0.214R$
$\text{H}_2\text{N}-\text{YH}_m$	86	$\%s = 112 - 22.0E - 0.256R$
$\text{HO}-\text{YH}_m$	79	$\%s = 120 - 24.9E - 0.316R$
$\text{F}-\text{YH}_m$	30	$\%s = 130 - 26.0E - 0.879R$

^a C_E and C_R are the coefficient in the fit equation that correlate hybridization with electronegativity (E) and size (R), respectively.

Hybridization in Nonpolar Bonds: Effects of Electron Promotion Energy. The nonpolar F–F and O–O bonds in the symmetric compounds are formed from almost pure p orbitals (5 and 12% of s character, respectively). In contrast, B–B, C–C, and N–N bonds are already substantially hybridized, even in the absence of polarization. The correlation between electron promotion energy and hybridization in Figure 12 illustrates that the unimportance of hybridization for F and O originates from the large atomic s–p gap that increases the energy cost for electron promotion.

Generally this energy cost is paid by the formation of new chemical bonds. As a consequence, a greater number of new bonds and the greater strength of the new bonds are the two factors which favor hybridization. Although these factors are relatively weak in F_2 and H_2O_2 , the strength of the new bonds

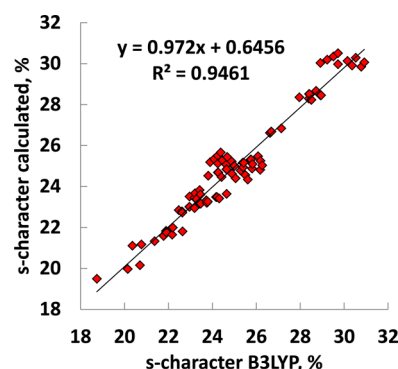


Figure 9. Comparison of optimized s character for chemical bonds in 35 halogenated methanes $\text{CA}_4\text{A}_1\text{A}_1\text{A}_1$ (substituents A: F, Cl, Br, and H) with s character calculated from eq 1 after determining A and B through fitting. Calculations are based on the B3LYP/6-311++G(d,p) data.

starts to increase as F and O form more polar bonds to less electronegative partners. As a consequence, the importance of hybridization in F–Y and O–Y bonds increases in parallel to the bond polarity.

Role of Nonbonding Orbitals: From Dative Bonds to Negative Hyperconjugation. Presence or absence of nonbonding orbitals (lone pairs) has a large impact on the ability to rehybridize (see Figure 13). In the absence of lone pairs (X = B and C), rehybridization in X–Y bonds is relatively small.

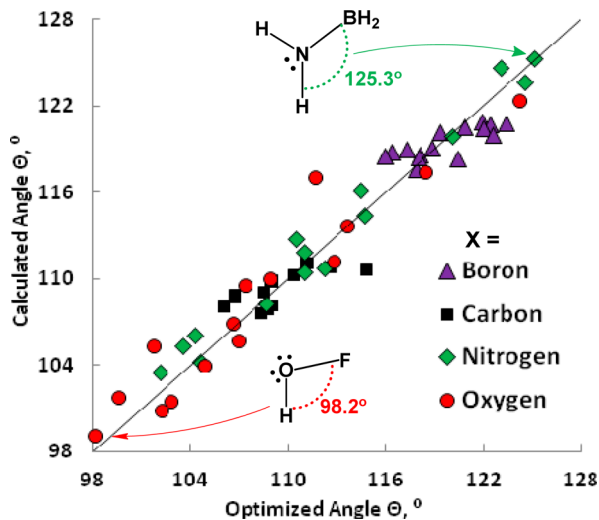


Figure 10. Comparison of valence angles Θ (H–X–Y) in geometry-optimized structures with angle Θ calculated from the s character at X in the X–Y and X–H bonds, using eq 2; MP2/6-311++G(d,p) level of theory.

In contrast, rehybridization is much larger for atoms with lone pairs (X = N, O, and F). The lone pairs provide a rehybridization resource, which can assist in reaching optimum hybridization of the covalent bonds.

The most direct effect of lone pairs is the formation of dative π bonds when an atom with a lone pair (N, O, F) is adjacent to the BH_2 moiety. This phenomenon explains the unusually high amount of s character in the X–B bonds observed for the elements X with lone pairs (the N–B, O–B, and F–B bonds). Formation of the additional π bond leads to different Lewis

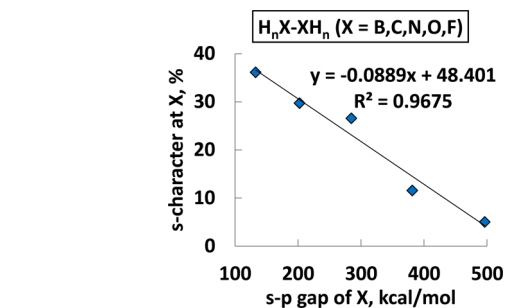


Figure 12. Hybridization in the absence of polarization: effects of the s–p gap for the 2nd period elements. Hybridization is provided by NBO analysis of the B3LYP/6-311++G(d,p)-optimized structures; s–p gaps are taken from ref 4. Similar linear correlations are found for the 3rd and 4th periods (see the Supporting Information section).

structures of such compounds and takes a p orbital out of the hybridization mix, thus increasing the average s character in the remaining three hybrids.

Smaller in magnitude but a conceptually analogous effect associated with the presence of lone pairs is negative hyperconjugation.⁹¹ Because hyperconjugation increases the double bond character between the central atoms (as illustrated by the resonance structure in Figure 14), it also affects molecular geometry and leads to partial rehybridization, “on route” to a dative π bond.

■ IMPACT OF ADDITIONAL BONDS: HYBRIDIZATION IN $\text{H}_n\text{X} = \text{YH}_m$ AND $\text{H}_n\text{X} \equiv \text{YH}_m$

The analysis of the unsaturated compounds revealed that double bonds generally form in the textbook-way: one π bond and a σ bond of varying s character.⁹² Analogously, the triple bonds have an additional π bond, of ~100% p character. Thus, for single-,

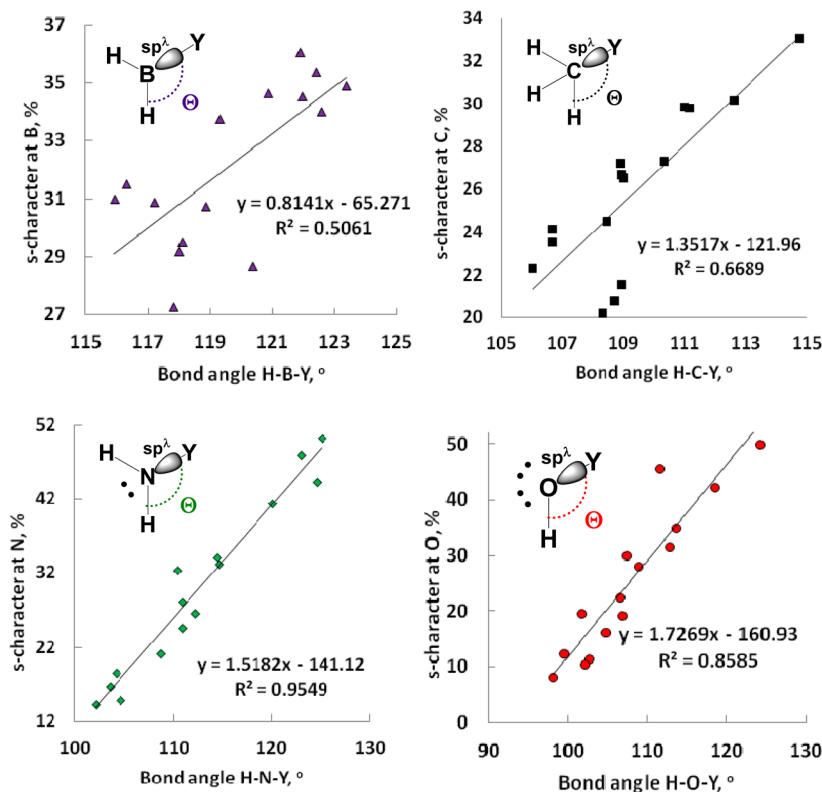


Figure 11. Correlation of bond angle Θ (H–X–Y) in $\text{H}_n\text{X}-\text{YH}_m$ ($\text{H}_n\text{X} = \text{H}_2\text{B}, \text{H}_3\text{C}, \text{H}_2\text{N}$, and HO) systems with the s character at X in the X–Y bond omitting hybridization changes in the X–H bonds; MP2/6-311++G(d,p) level of theory.

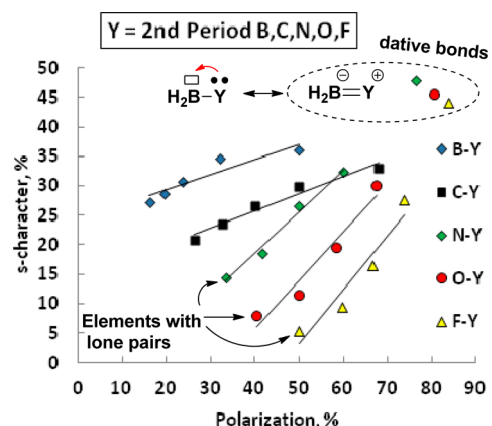


Figure 13. Illustration of the role of lone pairs. For atoms with lone pairs (N, O, and F), changes in polarization lead to much larger rehybridization than they do for B and C.

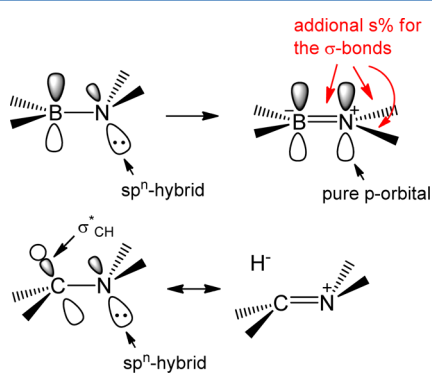


Figure 14. Top: The dative π bond removes one p orbital of nitrogen out of the hybridization mix in $\text{H}_2\text{B}=\text{NH}_2$. The remaining hybrid orbitals at nitrogen form σ bonds with a higher amount of s character. Bottom: Negative hyperconjugation increases the double bond character at atoms with a lone pair.

double-, and triple-bonded compounds, only the hybridization of the σ bond varies.

As shown in Figure 15, a comparison between the s character at atom X bound with single, double, and triple bonds to a

neighbor atom yields a linear dependence on the number of bonds up to the third bond; the higher the number of bonds, the higher the allocated s character in the σ bond. This pattern is maintained also for compounds bonded via a dative bond and is to be attributed to the fact that p orbitals are not available to mix, since they are occupied forming π bonds.

An interesting feature, however, is the difference in the extent of σ bond rehybridization for the C- and N-centered hybrids in these series, illustrated by the slopes of the four correlations in Figure 15. The N-centered hybrids in the σ bonds of unsaturated compounds gain s character slower than the respective C-centered hybrids and nitrogen lone pairs.

In the following sections, we will discuss several examples of unusual structural and electronic features originating from the interplay of hybridization effects with other factors. Our goal is to illustrate both the utility of hybridization and the limitations of this concept in the presence of stronger electronic effects.

Effect of Charge Introduction at the Adjacent Atom.

Introduction of charge changes the effective electronegativity, as illustrated by comparison of cationic, neutral, and anionic species in Figure 16. The cationic substituents have an effectively higher electronegativity than the neutral counterpart, and hence, less s character is used to form the bond toward the charged substituent. Inversely, this relationship could be used to formulate a definition for the electronegativity of ions, which we are not going to pursue in this work. Anionic behavior follows the opposite trend: less p character is allocated at X toward the substituent Y in the X–Y bond.

Hybridization effects readily explain the relative trend in H–C–H angles of methanol upon the protonation and deprotonation of the OH group. Whereas OH protonation increases the H–C–H angle from $\sim 109^\circ$ to $\sim 112^\circ$, OH deprotonation decreases the H–C–H angle to $\sim 102^\circ$. Although the effect of deprotonation is smaller than predicted by eq 2, an excellent linear correlation ($R^2 = 0.97$) between the angles derived from eq 2 and the NBO hybridization values, and the angles provided by geometry optimization, is observed. And even though the deviation from eq 2 indicate that additional factors are present, the good quality of this correlation confirms that hybridization is still a key effect, even in such charged molecules; while the almost identical correlation slopes for the different bonds suggest that

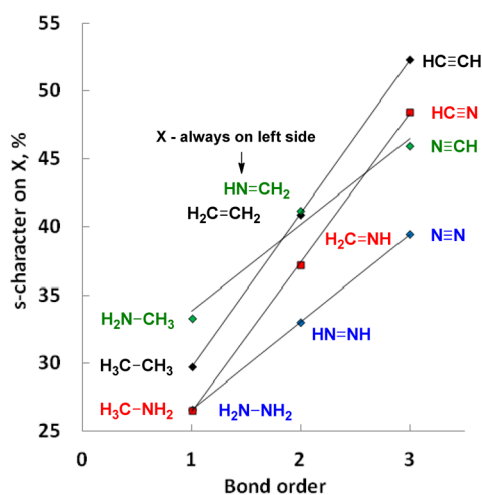
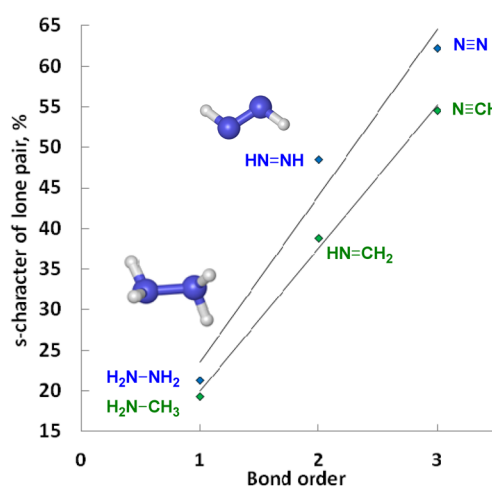


Figure 15. Left: Comparison of the s character at X allocated into the σ_{X-Y} bond for compounds containing single, double, and triple bonds between C and N atoms. Each additional π bond takes a complete p orbital out of the hybridization mix. The s character is shown always for the left central atom in each molecule. Right: Comparison of the s character allocated in lone pairs of nitrogen compounds. Calculations are at the B3LYP/6-311++G(d,p)-level. Full data are given in the Supporting Information.



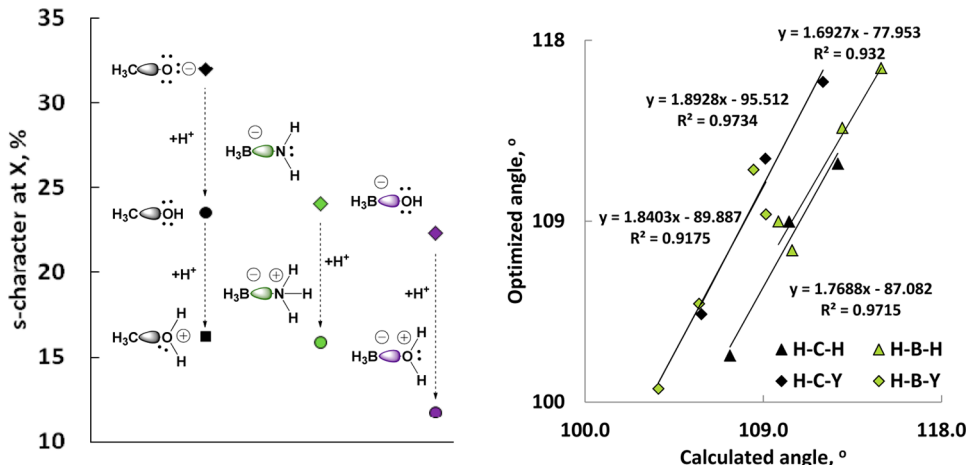


Figure 16. Left: Calculated s character at X in X-Y bonds for MeOH_2^+ , MeOH, MeO^- , $\text{BH}_3\text{-NH}_3^+$, $\text{BH}_3\text{-NH}_2$, $\text{BH}_3\text{-OH}_2^+$, and $\text{BH}_3\text{-OH}$ at the B3LYP/6-311++G^{**} level (X-Y: C–O, black; B–N, green; B–O, violet; anions, \blacklozenge ; neutral/zwitterion, \bullet , cations, \blacksquare). Right: Correlation of the bond angles using the calculated hybridization values (eq 2) with angles from full geometry optimization (description of the data labels is given on the plot).

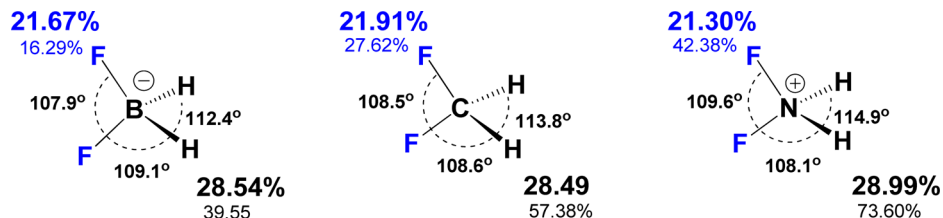


Figure 17. Hybridization (bold, top number), polarization (lower number), and bond angles for isoelectronic XF_2H_2 compounds. Calculations are at the B3LYP/6-311++G(d,p) level.

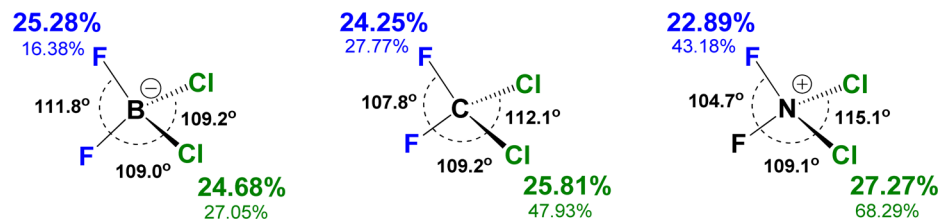


Figure 18. Hybridization (bold, top number), polarization (lower number), and bond angles for isoelectronic XF_2Cl_2 compounds. Calculations are at the B3LYP/6-311++G(d,p) level.

Table 4. Bond Lengths for XF_2H_2 Compounds^a

bond length (Å)	X = B ⁻	X = C	X = N ⁺
X–F	1.4547	1.3665	1.3434
X–H	1.2381	1.0913	1.0407

^aCalculations are at the B3LYP/6-311++G(d,p) level.

Table 5. Bond Lengths for XF_2Cl_2 Compounds at the B3LYP/6-311++G(d,p) Level

bond length (Å)	X = B ⁻	X = C	X = N ⁺
X–F	1.3846	1.3378	1.3577
X–Cl	1.9207	1.7792	1.7473

the additional factors that influence this correlation are the same for these molecular systems.

Rehybridization at Charged Centers: Tug-of-War between Electronegativity and Orbital Size Effects. In order to evaluate the scope and limitations of hybridization effects on the structure of main group compounds, we had investigated the interplay of hybridization and geometric features in isoelectronic compounds with different charges at the central

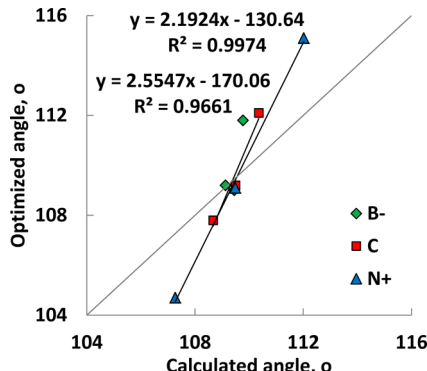


Figure 19. Comparison of all optimized angles and all angles calculated from the corresponding s characters in XF_2Cl_2 compounds in Figure 18.

atom. In particular, we tested whether the structural preferences in CH_2F_2 (angles: F–C–F < H–C–H) are transferrable to BF_2H_2^- and NF_2H_2^+ . Interestingly, neither hybridization nor the general trend in angles changed significantly, despite the very large differences in the bond polarities (from 84% of density at F

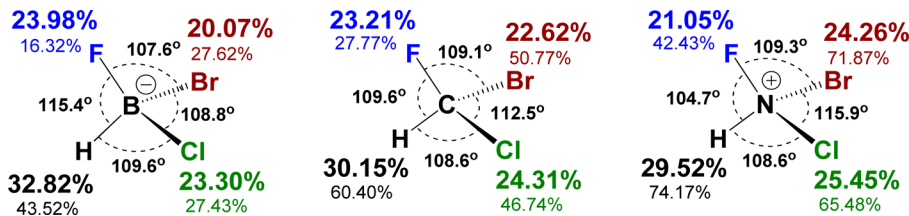


Figure 20. Similar s character distribution (bold, top number) but different polarizations (lower number) and geometries at the central atom in NHFClBr⁺, CHFClBr, and BHFClBr⁻. Hybridizations and geometries are based on the B3LYP/6-311++G(d,p) data.

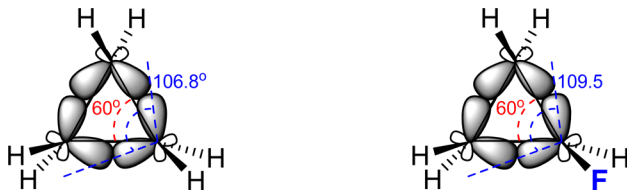


Figure 21. Unusual hybridization and bent bonds in cyclopropane (left) and further increase in bond bending upon the introduction of the fluorine atom. Orbital angle determined from s character in C–C bond using eq 1 after optimization at the B3LYP/6-311++G(d,p) level.

in the B–F bonds to 58% at F in the N–F bonds) and the dramatic contraction of both C–F and C–H bonds upon the transition from anionic to cationic central atom (Figure 17, Table 4). This trend suggests that it is not polarization per se but the difference in polarization that is responsible for the differences in hybridization and geometry. The shown hybridization patterns also

Table 6. Bond Lengths for XFClBrH Compounds^a

bond length (Å)	X = B ⁻	X = C	X = N ⁺
F–X	1.3856	1.3512	1.3789
Cl–X	1.9115	1.7785	1.7405
Br–X	2.1479	1.9587	1.9333
H–X	1.1971	1.0850	1.0320

^aCalculations are at the B3LYP/6-311++G(d,p) level.

justify approximation expressed by eq 1, which omits the electronegativity and the covalent radius of the central atom.

In order to evaluate how the charge effects control the competition between electronegativity and orbital size effects, we investigated the rivalry between X–F and X–Cl bonds as a function of charge at the central atom (Figure 18, Table 5). Although all of the observed angle changes still follow the altered distribution of s character, the effects here were much more

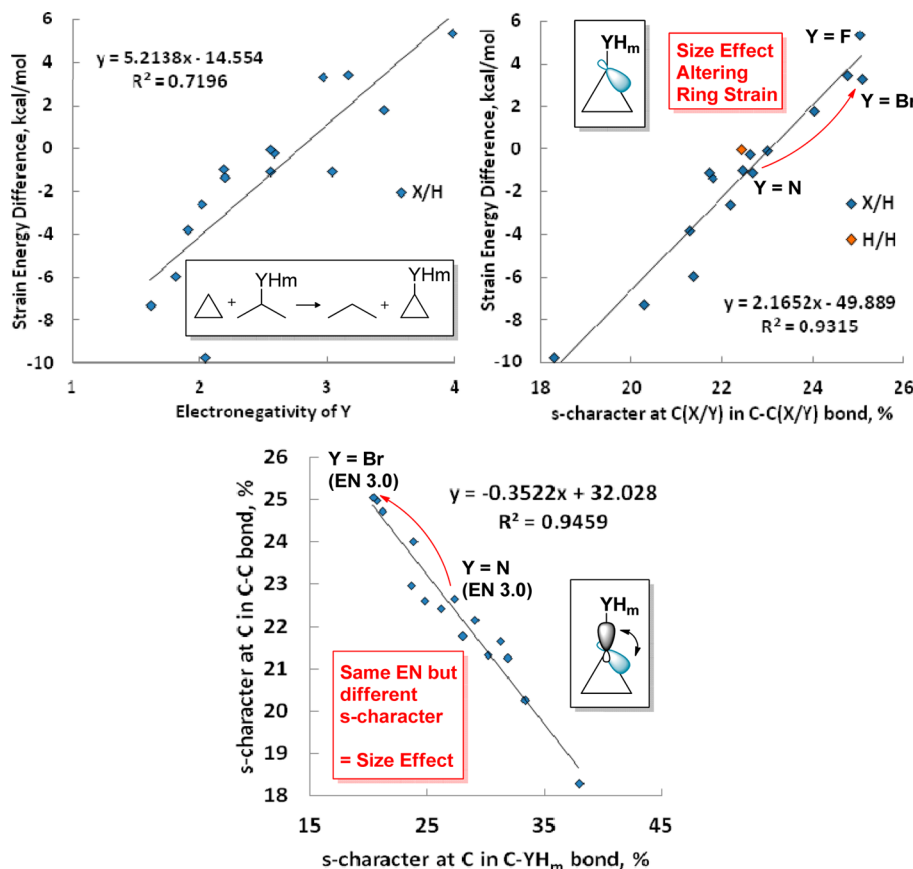


Figure 22. Correlation of relative strain energy in substituted cyclopropanes with electronegativity of Y (left) and s character at C in the C–C(YH_m) bond (right). The dependence of the strain energy difference on the s character in the C–C(YH_m) bonds in the cyclopropane cycle provides a clearer picture. The increased s character in the C–C bonds in the ring is clearly induced by the altered hybridization in the C–Y bond (bottom). Calculations are based on the B3LYP/6-311++G(d,p) data.

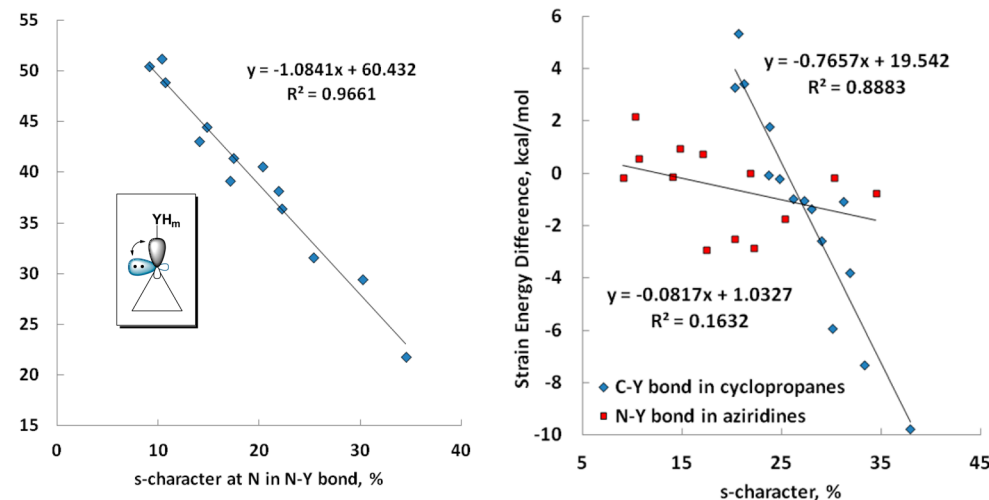


Figure 23. Left: The altered hybridization in the N–Y bond is compensated by rehybridization of the nitrogen lone pair (Y = group 14–17). Right: Comparison of the strain energy in aziridines and cyclopropanes as a function of the s character at C in the C– YH_m bonds and N in the N– YH_m bonds. Aziridines containing dative double bonds are omitted for clarity. Calculations are based on the B3LYP/6-311++G(d,p) data.

surprising. Whereas the F–X–F angle contracted from 112 to 105°, the Cl–X–Cl angle displayed an opposite transition (from 109 to 115°) as the central atom changed its formal charge from negative to positive. Remarkably, the trend for F–C–F angles in the XF_2Cl_2 series is the opposite of that in the XF_2H_2 series. This effect is similar to the large angle changes in Figure 16.

This difference suggests that the X–Cl bonds are more sensitive to the charge effects than the X–F bonds. As the result, in the anionic compound, the C–Cl bonds get more p character than the C–F bonds (this can be interpreted as the greater importance of the orbital size in comparison to the electronegativity effects). However, in the cationic complexes, it is the C–F bonds that get the more p character, suggesting that electronegativity trumps orbital size effects under the conditions of greater electron demand. Furthermore, the irregular trend in the F–X bonds (Table 5) suggests that hyperconjugative effects also change in an irregular way and may be important in more closely balanced situations.

As shown in Figure 19, the correlation between the actual (optimized) angles ($\text{A}–\text{X}–\text{B}$) from the angles that have been calculated using the s characters of corresponding bonds ($\text{X}–\text{A}$ and $\text{X}–\text{B}$) is similar to that in Figure 16 (right), suggesting the same effect is at work.

Finally, we evaluated the competition between four different elements of dramatically different electronegativities and sizes (Figure 20, Table 6). The situation here is very complex. In these systems, the simple version of the Bent's rule reached the limits of its predictive power. Clearly, one needs to incorporate the effects of dramatically different bond lengths, variations in the strengths of negative hyperconjugation, and perhaps the involvement of bent bonds in order to describe these seemingly irrational trends.

Use of Hybridization Effects for Strain Modulation. The connection between molecular geometry and hybridization can be used to modulate strain in cyclic compounds. Cyclopropane is a particularly unusual but also particularly useful cycle, where molecular geometry imposes unusual hybridization ($\sim\text{sp}^5$ in the Walsh model, $\text{sp}^{3.5}$ from NBO analysis) accompanied by the limited possibility of secondary effects (i.e., hyperconjugation) to influence the total energy and conformation of the molecule (see Figure 21). As a consequence of this unusual hybridization,

cyclopropanes should be particularly sensitive to rehybridization effects.

Indeed, Figure 22 illustrates that the scope of these effects in monosubstituted cyclopropanes is large. Interestingly, the correlation of strain energy with hybridization of C in the C–Y bond is better than the correlation with electronegativity of Y, providing a straightforward rationale for the very large (~16 kcal/mol) range of strain energies in this family of compounds.⁹³

In contrast to cyclopropanes, substituted aziridines allow much less of the ring strain engineering since the substituent-dependent rehybridization in the N–Y bond is easily compensated by rehybridization of the lone pair, leaving the two N–C bonds in the ring essentially unaltered (Figure 23). Only if the substituent is chosen out of the boron group an effective strain modulation is found, since the formed dative bond is removing the lone pair as an available rehybridization source.

CONCLUSION

Electronic analysis of H–Y bonds in 75 $\text{H}_n\text{X}–\text{YH}_m$ compounds made of five second period elements X (X = B, C, N, O, and F) and 15 elements Y from periods 2–4 found that although polarization in X–Y bonds depends linearly on the electronegativity, hybridization follows a more complicated trend, where the effect of electronegativity is complemented by the effect of the covalent radius. Bonds from X to larger elements Y from the later periods are allocated more p character than could be anticipated from electronegativity of Y.

When the correlation electronegativity and hybridization is extended by inclusion of a linear term corresponding to the covalent radius of element Y, a good two-parameter global correlation exists. This finding expands the Bent's rule toward most elements of the second period (groups III–VII) in the following way: “An atom distributes its p character into the bonds toward its substituents dependent on their electronegativity and covalent radius. The bigger and more electronegative a substituent, the more p character will be incorporated into this elements bond.”

The rehybridization range of elements with lone pairs (N, O, and F) is considerably larger than for elements without lone pairs (B and C). In particular, although the nonpolar O–O and F–F

bonds are made from almost pure p orbitals (consequence of the relatively large s–p gap), the polarity of O–Y and F–Y bonds increases the importance of hybridization. As the result, valence hybrids at F in F–Y bonds changed from sp^{19} (F–F) to sp^3 (F–C) orbitals. The “super-rehybridization” is facilitated by the lower penalty for rehybridization in nonbonding orbitals. This phenomenon accounts for the greater changes in valence angles in compounds with lone pairs.

The distribution of s character between bonds on a multi-substituted atom can be described with the symmetry derived eq 1, where the competition of the substituents for p character of the central atom is a tug-of-war in which each substituent holds its electronegativity against the average of the electronegativities and covalent radii effects of other substituents. A substituent will gain less s character when the average electronegativity and the average covalent radii of the other substituents decrease.

The relative importance of electronegativity and orbital size is not set in stone and can change upon the conditions of varying electronic demand, as illustrated by the trends in ionic species. In particular, in the case of increased electron demand, hybridization evolves in a systematic way where orbital size effects seem to gradually become more important than electronegativity (i.e., in several investigated systems, the more polarizable bonds to heavier elements responded stronger to the effects of charge introduction).

Because bonds from X to larger elements Y of the later periods are allocated more p character than could be anticipated from electronegativity of Y, one can change hybridization without changes in polarization. This finding provides an alternative way to control geometries, energies, and reactivities for molecules formed from the main group elements. This notion is illustrated by the strong correlation of strain effects in monosubstituted cyclopropanes with hybridization in the bond to the substituent. On the other hand, the “super-rehybridization”, characteristic for atoms with a lone pair (i.e., nitrogen atom of aziridines) can remove most of strain associated with introduction of acceptor and large substituents in three-membered rings.

Overall, hybridization cannot provide answers to all structural and electronics questions but it continues to serve as one of the key pieces needed for unraveling the future puzzles of molecular structure and reactivity.

ASSOCIATED CONTENT

Supporting Information

Polarization, hybridization, Cartesian coordinates, and total energies for all optimized geometries at different levels of theory. Two variable fits correlating hybridization of atom X with electronegativity and covalent radius of atom Y. Optimized bond angles, calculated bond angles, and bond length for selected compounds. Strain energy differences for substituted cyclopropane. Hybridization/s–p gap plots. Additional references. This material is available free of charge via the Internet at <http://pubs.acs.org>.

AUTHOR INFORMATION

Corresponding Author

*E-mail: alabugin@chem.fsu.edu.

Notes

The authors declare no competing financial interest.

ACKNOWLEDGMENTS

Financial support by NSF (Grant CHE-1152491) is gratefully acknowledged. We are grateful to Professors Wes Borden (UNT) and Roald Hoffmann (Cornell) for helpful discussions.

REFERENCES

- (1) Pauling, L. The nature of the chemical bond. Application of results obtained from the quantum mechanics and from a theory of paramagnetic susceptibility to the structure of molecules. *J. Am. Chem. Soc.* **1931**, *53*, 1367–1400.
- (2) Pauling, L. *The Nature of the Chemical Bond*; Cornell University Press: Ithaca, NY, 1960.
- (3) The percentage of s character and the hybridization parameter λ are linked through the two equivalent equations: $100/(\lambda + 1) = \% \text{ s}$ and $\% \text{ p}/\lambda = \% \text{ s}$.
- (4) Allen, L. C. Electronegativity is the average one-electron energy of the valence-shell electrons in ground-state free atoms. *J. Am. Chem. Soc.* **1989**, *111*, 9003–9014.
- (5) Alabugin, I. V. Stereoelectronic interactions in cyclohexane, 1,3-dioxane, 1,3-oxathiane, and 1,3-dithiane: W-effect, $\sigma_{\text{C}-\text{X}} \leftrightarrow \sigma^*_{\text{C}-\text{H}}$ interactions, anomeric effect what is really important? *J. Org. Chem.* **2000**, *65*, 3910–3919.
- (6) Grushow, A. Is it time to retire the hybrid atomic orbital? *J. Chem. Educ.* **2011**, *88* (7), 860–862.
- (7) Grushow, A. In response to those who wish to retain hybrid atomic orbitals in the curriculum. *J. Chem. Educ.* **2012**, *89* (5), 578.
- (8) Hiberty, P. C.; Volatron, F.; Shaik, S. In defense of the hybrid atomic orbitals. *J. Chem. Educ.* **2012**, *89*, 575–577.
- (9) Tro, N. J. Retire the hybrid atomic orbital? Not so fast. *J. Chem. Educ.* **2012**, *89*, 567–568.
- (10) DeKock, R. L. Retire hybrid atomic orbitals? *J. Chem. Educ.* **2012**, *89* (5), 569–569.
- (11) Landis, C. R.; Weinhold, F. Comments on “Is it time to retire the hybrid atomic orbital?” *J. Chem. Educ.* **2012**, *89*, 570–572.
- (12) Alabugin, I. V.; Manoharan, M.; Peabody, S.; Weinhold, F. The electronic basis of improper hydrogen bonding: A subtle balance of hyperconjugation and rehybridization. *J. Am. Chem. Soc.* **2003**, *125*, 5973–5987.
- (13) Alabugin, I. V.; Manoharan, M. Rehybridization as a general mechanism for maximizing chemical and supramolecular bonding and a driving force for chemical reactions. *J. Comput. Chem.* **2007**, *28*, 373–390.
- (14) Andujar-De Sanctis, I. L.; Singleton, D. A. Racing carbon atoms. atomic motion reaction coordinates and structural effects on newtonian kinetic isotope effects. *Org. Lett.* **2012**, *14*, 5238–5241.
- (15) Kelly, K. K.; Hirschi, J. S.; Singleton, D. A. Newtonian kinetic isotope effects. observation, prediction, and origin of heavy-atom dynamic isotope effects. *J. Am. Chem. Soc.* **2009**, *131*, 8382–8383.
- (16) Hammann, B.; Razzaghi, M.; Kashefolgheta, S.; Lu, Y. Imbalanced tunneling ready states in alcohol dehydrogenase model reactions: Rehybridization lags behind H-tunneling. *Chem. Commun.* **2012**, *48*, 11337–11339.
- (17) MacMillar, S.; Edmondson, D. E.; Matsson, O. Nitrogen kinetic isotope effects for the monoamine oxidase B-catalyzed oxidation of benzylamine and (1,1- H_2)benzylamine: Nitrogen rehybridization and CH bond cleavage are not concerted. *J. Am. Chem. Soc.* **2011**, *133*, 12319–12321.
- (18) Bent, H. A. Electronegativities from comparison of bond lengths in AH and AH⁺. *J. Chem. Phys.* **1959**, *33*, 1258–1258.
- (19) Bent, H. A. Distribution of atomic s character in molecules and its chemical implications. *J. Chem. Educ.* **1960**, *37*, 616–624.
- (20) Bent, H. A. An appraisal of valence-bond structures and hybridization in compounds of the first-row elements. *Chem. Rev.* **1961**, *61*, 275–311.
- (21) Streitwieser, A.; Ziegler, G. R.; Mowey, P. C.; Lewis, A.; Lawler, R. G. Some generalizations concerning the reactivity of aryl positions adjacent to fused strained rings. *J. Am. Chem. Soc.* **1968**, *90*, 1357–1358.

- (22) Haddon, R. C. Rehybridization and π -orbital overlap in nonplanar conjugated organic molecules: π -orbital axis vector (POAV) analysis and three-dimensional Hueckel molecular orbital (3D-HMO) theory. *J. Am. Chem. Soc.* **1987**, *109*, 1676–1685.
- (23) Carpenter, J. E.; Weinhold, F. Transferability of natural bond orbitals. *J. Am. Chem. Soc.* **1988**, *110*, 368–372.
- (24) Faust, R.; Glendening, E. D.; Streitwieser, A.; Vollhardt, P. C. b initio study of σ - and π -effects in benzenes fused to four-membered rings: Rehybridization, delocalization, and antiaromaticity. *J. Am. Chem. Soc.* **1992**, *114*, 8263–8268.
- (25) Major, D. T.; York, D. M.; Gao, J. Solvent polarization and kinetic isotope effects in nitroethane deprotonation and implications to the nitroalkane oxidase reaction. *J. Am. Chem. Soc.* **2005**, *127*, 16374–16375.
- (26) Mo, Y.; Lin, Z.; Wu, W.; Zhang, Q. Delocalization in allyl cation, radical, and anion. *J. Phys. Chem.* **1996**, *100* (16), 6469–6474.
- (27) Lauvergnat, D.; Maitre, P.; Hiberty, P. C.; Volatron, F. Valence bond analysis of the lone pair bond weakening effect for the X–H bonds in the series $XH_n = CH_4, NH_3, OH_2, FH$. *J. Phys. Chem.* **1996**, *100*, 6463–6468.
- (28) Eckert-Maksić; Glasovac, Z.; Hodošček, M.; Lesar, A.; Maksić, Z. B. Molecular and electronic structure of 1,2-disilacyclobutabenzenes. Ab initio molecular orbital and density functional study. *J. Organomet. Chem.* **1996**, *524* (1–2), 107–114.
- (29) Merrill, P. B.; Madix, R. J. Hydrogenation of weakly rehybridized ethylene on Fe(100)–h: ethyl group formation. *J. Am. Chem. Soc.* **1996**, *118*, 5062–5067.
- (30) Skancke, A.; Skancke, P. N. Density functional theory and perturbation calculations on some lewis acid–base complexes. A systematic study of substitution effects. *J. Phys. Chem.* **1996**, *100*, 15079–15082.
- (31) Worthington, S. E.; Cramer, C. J. Density functional calculations of the influence of substitution on singlet–triplet gaps in carbenes and vinylidenes. *J. Phys. Org. Chem.* **1997**, *10*, 755–757.
- (32) Palmer, M. H. Deviations from idealised geometries part 4: Approximately tetrahedral molecules of form MX_2Y_2 studied by SCF and MP2 localised orbital calculations. *J. Mol. Struct.* **1997**, *40S*, 193–205.
- (33) Ou, M. C.; Chu, S. Y. Rehybridization in annelated benzene and dissociating glyoxal. *J. Mol. Struct. (Theochem)* **1997**, *401*, 87–92.
- (34) Lewis, B. E.; Schramm, V. L. Conformational equilibrium isotope effects in glucose by ^{13}C NMR spectroscopy and computational studies. *J. Am. Chem. Soc.* **2001**, *123*, 1327–1336.
- (35) Krygowski, T. M.; Pindelska, E.; Crysński, M. K.; Häfleinger, G. Planarization of 1,3,5,7-cyclooctatetraene as a result of a partial rehybridization at carbon atoms: An MP2/6-31G* and B3LYP/6-311G** study. *Chem. Phys. Lett.* **2002**, *359*, 158–162.
- (36) Oxgaard, J.; Wiest, O. Rehybridized 1,3-butadiene radical cations: How far will a radical cation go to maintain conjugation? *J. Phys. Chem. A* **2002**, *106*, 3967–3974.
- (37) Baldridge, K. K.; Siegel, J. S. Directing power of cyclobutenoid annelations on the double bonds of planar cyclooctatetraenes. *J. Am. Chem. Soc.* **2002**, *124*, 5514–5517.
- (38) Öström, H.; Triguero, L.; Weiss, K.; Ogasawara, H.; Garnier, M. G.; Nordlund, D.; Nyberg, M.; Pettersson, L. G. M.; Nilsson, A. Orbital rehybridization in n-octane adsorbed on Cu(110). *J. Chem. Phys.* **2003**, *118*, 3782–3790.
- (39) Clark, A. E.; Davidson, E. R. *p*-Benzyne derivatives that have exceptionally small singlet–triplet gaps and even a triplet ground state. *J. Org. Chem.* **2003**, *68*, 3387–3396.
- (40) Alabugin, I. V.; Manoharan, M.; Zeidan, T. A. Homoanomeric effects in six-membered heterocycles. *J. Am. Chem. Soc.* **2003**, *125*, 14014–14031.
- (41) Donald, K. J.; Böhm, M. C.; Lindner, H. J. Analysis of competing bonding parameters. Part 2. The structure of halosilanes and halogermanes ($MH_{4-n}X_n$, $n = 1–4$; M=Si, Ge; X=F, Cl, Br). *J. Mol. Struct. (Theochem)* **2005**, *713*, 215–226.
- (42) Lin, T.; Zhang, W. D.; Huang, J.; He, C. A DFT study of the amination of fullerenes and carbon nanotubes: Reactivity and curvature. *J. Phys. Chem. B* **2005**, *109*, 13755–13760.
- (43) In clusters: Jemmis, E. D.; Parameswaran, P.; Anoop, A. Effect of metal complexation on ring opening of bowl-shaped hydrocarbons: Theoretical study. *Int. J. Quantum Chem.* **2003**, *95*, 810–815.
- (44) Pu, J.; Ma, S.; Garcia-Viloca, M.; Gao, J.; Truhlar, D. G.; Kohen, A. Nonperfect synchronization of reaction center rehybridization in the transition state of the hydride transfer catalyzed by dihydrofolate reductase. *J. Am. Chem. Soc.* **2005**, *127*, 14879–14886.
- (45) Hamon, M. A.; Itkis, M. E.; Alvarez, T.; Kuper, C.; Menon, M.; Haddon, R. C. Effect of rehybridization on the electronic structure of single-walled carbon nanotubes. *J. Am. Chem. Soc.* **2001**, *123*, 11292–11293.
- (46) In reactions: Lewis, M.; Glaser, R. Synergism of catalysis and reaction center rehybridization. An ab initio study of the hydrolysis of the parent carbodiimide. *J. Am. Chem. Soc.* **1998**, *120*, 8541–8542.
- (47) Lewis, M.; Glaser, R. Synergism of catalysis and reaction center rehybridization. A novel mode of catalysis in the hydrolysis of carbon dioxide. *J. Phys. Chem. A* **2003**, *107*, 6814–6818.
- (48) Norberg, D.; Larsson, P. E.; Dong, X. C.; Salhi-Benachenhou, N.; Lunell, S. Bicyclopropylidene radical cation: A rehybridization ring opening to tetramethyleneethane. *Int. J. Quantum Chem.* **2004**, *98*, 473–483.
- (49) Mohamed, R. K.; Peterson, P. W.; Alabugin, I. V. Concerted reactions that produce diradicals and zwitterions: Electronic, steric, conformational, and kinetic control of cycloaromatization processes. *Chem. Rev.* **2013**, *113*, 7089–7112.
- (50) Gold, B.; Dudley, G. B.; Alabugin, I. V. Moderating strain without sacrificing reactivity: Design of fast and tunable noncatalyzed alkyne–azide cycloadditions via stereoelectronically controlled transition state stabilization. *J. Am. Chem. Soc.* **2013**, *135*, 1558.
- (51) “Two functional groups in one package”: Designing cascade transformations of alkynes. Alabugin, I. V.; Gold, B. *J. Org. Chem.* **2013**, *78*, 7777–7784.
- (52) For a particularly instructive selection of rehybridization effects in reactivity of fluoroorganic compounds, see: O’Hagan, D. Understanding Organofluorine Chemistry. An Introduction to the C–F Bond. *Chem. Soc. Rev.* **2008**, *37*, 308–319.
- (53) Foster, J. P.; Weinhold, F. Natural hybrid orbitals. *J. Am. Chem. Soc.* **1980**, *102*, 7211–7218.
- (54) Huheey, J. E. Bent’s rule: Energetics, electronegativity, and the structures of nonmetal fluorides. *Inorg. Chem.* **1981**, *20*, 4033–4035.
- (55) Kaupp, M.; Schleyer, P. v. R. Ab initio study of structures and stabilities of substituted lead compounds. Why is inorganic lead chemistry dominated by PbII but organolead chemistry by Pb(IV)? *J. Am. Chem. Soc.* **1993**, *115*, 1061–1073.
- (56) Root, D. M.; Landis, C. R.; Cleveland, T. Valence bond concepts applied to the molecular mechanics description of molecular shapes. 1. Application to nonhypervalent molecules of the P-block. *J. Am. Chem. Soc.* **1993**, *115*, 4201–4209.
- (57) Jonas, V.; Boehme, C.; Frenking, G. Bent’s rule and the structure of transition metal compounds. *Inorg. Chem.* **1996**, *35*, 2097–2099.
- (58) Kaupp, M. On the relation between π -bonding, electronegativity, and bond angles in high-valent transition metal complexes. *Chem.—Eur. J.* **1999**, *5*, 3631–3643.
- (59) Lemke, F. R.; Galat, K. J.; Youngs, W. J. Ruthenium silyl complexes containing the $Cp(PMe_3)_2Ru$ moiety: Preparation, substituent effects, and silylene character in the Ru–Si bond. *Organometallics* **1999**, *18*, 1419–1429.
- (60) Kaupp, M. Non-VSEPR” structures and bonding in d^0 systems. *Angew. Chem., Int. Ed.* **2001**, *40*, 3534–3565.
- (61) Ghosh, D. C.; Bhattacharyya, S. Computation of quantum mechanical hybridization and dipole correlation of the electronic structure of the F_3B-NH_3 supermolecule. *Int. J. Quantum Chem.* **2005**, *105*, 270–279.
- (62) Alabugin, I. V.; Manoharan, M.; Buck, M.; Clark, R. Substituted anilines: The tug-of-war between pyramidalization and resonance inside

- and outside of crystal cavities. *J. Mol. Struct. (THEOCHEM)* **2007**, *813*, 21–27.
- (63) Ferbinteanu, M.; Roesky, H. W.; Cimpoesu, F.; Atanasov, M.; Kopke, S.; Herbst-Irmer, R. New Synthetic and structural aspects in the chemistry of alkylaluminum fluorides. the mutual influence of hard and soft ligands and the hybridization as rigorous structural criterion. *Inorg. Chem.* **2001**, *40*, 4947–4955.
- (64) Kirschenbaum, L. J.; Ruekberg, B. Relating bond angles of dihalo- and tetrahydro-methanes, -silanes, and -germanes to electronegativities. *J. Chem. Educ.* **2012**, *89*, 351–354.
- (65) We deliberately did not include hypervalent compounds where hybridization is not well-defined and arguments based on this concept may be misleading: Wang, J.-T.; Feng, Y.; Liu, L.; Li, X.-S.; Guo, Q.-X. Blue-shifted hydrogen bonds with proton-donors incapable of rehybridization. *Chem. Lett.* **2003**, *32*, 746–747.
- (66) Alabugin, I. V.; Manoharan, M.; Weinhold, F. Blue-shifted and red-shifted hydrogen bonds in hypervalent rare-gas FRg–H···Y sandwiches. *J. Phys. Chem. A* **2004**, *108*, 4720.
- (67) Frisch, M. J.; et al. *Gaussian 03*, revision E.01; Gaussian, Inc.: Wallingford, CT, 2004.
- (68) Frisch, M. J.; et al. *Gaussian 09*, revision C.01; Gaussian, Inc.: Wallingford, CT, 2009.
- (69) We use the most stable conformations throughout the paper even though this might involve additional effects on hybridization through distortion via hyperconjugation or steric repulsion that could be avoided by using less stable conformers.
- (70) For an illustrative rather than an exhaustive list of recent applications of the NBO method for analysis of chemical bonding see: Reed, A. E.; Weinhold, F. Natural bond orbital analysis of internal rotation barriers and related phenomena. *Isr. J. Chem.* **1991**, *31*, 277–285.
- (71) Goodman, L.; Popovits, V. T. Hyperconjugation not steric repulsion leads to the staggered structure of ethane. *Nature* **2001**, *411*, 565.
- (72) Salzner, U.; Schleyer, P. v. R. Ab initio examination of anomeric effects in tetrahydropyrans, 1,3-dioxanes, and glucose. *J. Org. Chem.* **1994**, *59*, 2138–2155.
- (73) Gleiter, R.; Lange, H.; Borzyk, O. Photoelectron spectra, ab initio scf mo, and natural bond orbital studies on stellenes. Long-range π/σ interactions. *J. Am. Chem. Soc.* **1996**, *118*, 4889–4895.
- (74) Klod, S.; Koch, A.; Kleinpeter, E. Ab-initio quantum-mechanical GIAO calculation of the anisotropic effect of C–C and X–C single bonds: Application to the ^1H NMR spectrum of cyclohexane. *J. Chem. Soc., Perkin Trans. 2* **2002**, *2*, 1506–1509.
- (75) Wilkens, S. J.; Westler, W. M.; Weinhold, F.; Markley, J. L. Trans-hydrogen bond $^{12}\text{J}_{\text{NN}}$ and $^{1\text{H}}\text{J}_{\text{NH}}$ couplings in the DNA A–T base pair: Natural bond orbital analysis. *J. Am. Chem. Soc.* **2002**, *124*, 1190–1191.
- (76) van der Veken, B. J.; Herrebout, W. A.; Szostak, R.; Shchepkin, D. N.; Havlas, Z.; Hobza, P. The nature of improper, blue-shifting hydrogen bonding verified experimentally. *J. Am. Chem. Soc.* **2001**, *123*, 12290–12293.
- (77) Cortes, F.; Tenorio, J.; Collera, O.; Cuevas, G. Electronic delocalization contribution to the anomeric effect evaluated by computational methods. *J. Org. Chem.* **2001**, *66*, 2918–2924.
- (78) Sadlej-Sosnowska, N. Application of natural bond orbital analysis to delocalization and aromaticity in C-substituted tetrazoles. *J. Org. Chem.* **2001**, *66*, 8737.
- (79) Uddin, J.; Boehme, C.; Frenking, G. Nature of the chemical bond between a transition metal and a group-13 element: Structure and bonding of transition metal complexes with terminal group-13 diyl ligands ER (E = B to Tl; R = Cp, N(SiH₃)₂, Ph, Me). *Organometallics* **2000**, *19*, 571–582.
- (80) Gilbert, T. M. Ab initio computational studies of heterocycloalkynes: Structures, natural bond orders, ring strain energies, and isomerizations of cyclic iminoboranes and iminoalanes. *Organometallics* **2000**, *19*, 1160.
- (81) Munoz, J.; Sponer, J.; Hobza, P.; Orozco, M.; Luque, F. J. Interactions of hydrated Mg²⁺ cation with bases, base pairs, and nucleotides. Electron topology, natural bond orbital, electrostatic, and vibrational study. *J. Phys. Chem. B* **2001**, *105*, 6051.
- (82) Xie, Y.; Grev, R. S.; Gu, J.; Schaefer, H. F., III; Schleyer, P. v. R.; Su, J.; Li, X.-W.; Robinson, G. H. The nature of the gallium–gallium triple bond. *J. Am. Chem. Soc.* **1998**, *120*, 3773–3780.
- (83) Paddon-Row, M. N.; Shephard, M. J. Through-bond orbital coupling, the parity rule, and the design of “superbridges” which exhibit greatly enhanced electronic coupling: A natural bond orbital analysis. *J. Am. Chem. Soc.* **1997**, *119*, 5355–5365.
- (84) Glendening, E. D.; Badenhoop, J. K.; Reed, A. E.; Carpenter, J. E.; Weinhold, F. NBO 4.0; Theoretical Chemistry Institute, University of Wisconsin: Madison, WI, 1996.
- (85) Reed, A. E.; Curtiss, L. A.; Weinhold, F. Intermolecular interactions from a natural bond orbital, donor-acceptor viewpoint. *Chem. Rev.* **1988**, *88*, 899–926.
- (86) Weinhold, F. *Encyclopedia of Computational Chemistry*; In Schleyer, P. v. R., Ed.; Wiley: New-York, 1998; Vol. 3, p 1792.
- (87) Reed, A. E.; Weinhold, F. Natural localized molecular orbitals. *J. Chem. Phys.* **1985**, *83*, 1736–1740.
- (88) We used the Pauling electronegativity scale.
- (89) Weinhold, F.; Landis, C. R. *Valency and Bonding: A Natural Bond Orbital Donor-Acceptor Perspective*; Cambridge University Press: Cambridge, 2005.
- (90) Deslongchamps, G.; Deslongchamps, P. Bent bonds and the antiperiplanar hypothesis as a simple model to predict diels–alder reactivity: Retrospective or perspective? *Tetrahedron* **2013**, *69*, 6022–6033.
- (91) Alabugin, I. V.; Gilmore, K.; Peterson, P. Hyperconjugation. *Wiley Interdiscip. Rev.: Comput. Mol. Sci.* **2011**, *1*, 109.
- (92) This is not always the case. See, for example, ref 13.
- (93) It will be interesting to estimate how such effects will be manifested in larger cycles capable of adjusting much better to the hybridization requirements than cyclopropane. Consequently, the range of strain energies in the larger cycles will be lower and dependence on hybridization should be weaker. We plan to investigate this connection in future work.